

Predicting the Binding Modes of SRI-3072 Inhibitor to *Mycobacterium tuberculosis* FtsZ using Docking and Molecular Dynamics Simulations

K. Sheranaravenich¹, S. Chongruchiroj¹, J. Pratuangdejkul^{1*}

¹Department of Microbiology, Faculty of Pharmacy, Mahidol University, Bangkok, Thailand

Abstract

To overcome the problem of multidrug-resistant (MDR) strains of *Mycobacterium tuberculosis* (Mtb) for tuberculosis (TB) treatment, there is an urgent need to identify new target and lead compound which have potential to develop as new anti-tuberculosis (anti-TB) drug. We are interested in protein that plays a crucial role in bacterial cell division, filamentous temperature-sensitive protein Z (FtsZ). The 2-alkoxycarbonylaminopyridine SRI-3072 has been reported as an anti-FtsZ agent that inhibits GTPase activity, FtsZ polymerization and growth of *M. tuberculosis* without any perturbation on tubulin. In this study, the structural insight into binding mode of SRI-3072 in MtbFtsZ was predicted using molecular modeling. The 3D-structure of MtbFtsZ (PDB code 1RLU) after deleting GTP- γ -S was used throughout this study. Two plausible binding sites of MtbFtsZ *i.e.* nucleotide-binding pocket and analogous Taxol-binding cleft were detected and applied for docking of SRI-3072. Base on top-ranked docking score and binding energy, pose-25 and pose-3 were selected to represent the binding modes of SRI-3072 in nucleotide-binding pocket and analogous Taxol-binding pocket of MtbFtsZ, respectively. The binding mode analyses of two stable complexes were deduced from molecular dynamics simulation. The types of interactions (*e.g.* hydrophobic, hydrogen bond) and interaction energies (*i.e.* van der Waals and electrostatic terms) were identified to allocate possible binding mode of SRI-3072. The results show that the preferable binding mode of SRI-3072 is in nucleotide-binding site as observed by the presence of strong binding energy and interactions. Our study provides structural information of MtbFtsz–SRI-3072 complex to be used as a tool for virtual screening, discovery and design of new anti-TB in the future.

Key words: SRI-3072, tuberculosis, FtsZ, docking, molecular dynamics, binding site

*Corresponding author: Department of Microbiology, Faculty of Pharmacy, Mahidol University, 447 Sri Ayudthaya Road, Rajthevi, Bangkok, 10400, Thailand. Tel.: +66 2644 8677 ext. 1133; fax: +66 2644 8692
E-mail address: pyjpd@mahidol.ac.th

INTRODUCTION

Tuberculosis (TB) remains the leading cause of worldwide death and common opportunistic infection for immunocompromised host such as HIV/AIDS patients. *Mycobacterium tuberculosis* (Mtb) is a causative bacterium for TB disease, and the number of infections has not declined. Poor anti-TB drug compliance has led to the emergence of multidrug-resistant (MDR) strains of Mtb. Therefore, discovery and development of anti-TB drugs with novel mechanism of action is required. Filamentous temperature-sensitive protein Z (FtsZ) is recently considerable as a new target for anti-bacterial drug discovery. FtsZ is a eukaryotic tubulin homolog which plays an essential role in bacterial cell-division. Z-ring formation of bacterial septum can be controlled by regulating intracellular FtsZ polymerization¹⁻⁴. FtsZ is conserved in bacteria and does not appear in human cell. Thus, FtsZ-inhibitors can be developed as antibacterial drugs without any perturbation on human host cell. At present, several FtsZ inhibitors were explored to develop as potential anti-TB agents. The inhibitors of MtbFtsZ have been reported so far to date, e.g. totarol, albendazole, thiabendazole, taxanes, benzimidazoles, 2-alkoxycarbonylaminopyridines and 2-carbamoylpteridine⁵.

In this study, we focus our attention on compound SRI-3072, a 2-alkoxycarbonylaminopyridine which inhibits FtsZ polymerization and growth of *M. tuberculosis* H37Rv without any perturbation on polymerization of bovine brain tubulin⁶⁻⁷. The structure of SRI-3072 is shown in Figure 1(a) and 1(b). SRI-3072 inhibited the growth of Mtb cells at concentration of 0.15 g/ml, inhibited MtbFtsZ polymerization in a dose-dependent manner with ID₅₀ values of 52 μ M and also inhibited the GTPase activity by 20–25% at concentration of 100 μ M⁶. Because SRI-3072 was specific to FtsZ, thus it has potential to develop into new anti-TB drugs effective against the current MDR strains of *M. tuberculosis*. Until now, there is no experimental structure available for give insight into the

MtbFtsZ–SRI-3072 interactions. In an attempt to reveal the binding mode of SRI-3072 with active site of FtsZ, the molecular interactions of SRI-3072 with MtbFtsZ can be investigated using molecular modeling techniques. Fortunately, the crystal structure of MtbFtsZ in complex with citrate, GDP and GTP- γ -S were successfully elucidated⁸. Structure of dimeric Mtb FtsZ reveals a tight and laterally orientation which is different from the longitudinal or head-to-tail polymer observed for $\alpha\beta$ -tubulin and crystal structure of FtsZ obtained from other bacterial species, e.g. *Aquifex aeolicus*, *Bacillus subtilis*, *Methanococcus jannaschii*, *Pseudomonas aeruginosa*⁸⁻⁹. The lateral association of dimeric MtbFtsZ in complex with GTP- γ -S (PDB code 1RLU) is shown in Figure 1(c). There is an evidence confirms that the mutations in lateral amino are critical to proper Z-ring formation and functionality¹⁰. From available structure of MtbFtsZ, the interaction of SRI-3072 with catalytic core domain of MtbFtsZ could be deduced by computational docking and molecular dynamics simulation. Our predicted structure exhibits the plausible binding site and binding mode of SRI-3072. The docked pose and trajectories obtained from molecular dynamics simulation were analyzed to validate the binding mode of SRI-3072 in Mtb FtsZ. Non-bonded interactions were analyzed in order to identify the structural features of SRI-3072 involved in binding interactions with active site FtsZ-residues. Our results shed light on the structural information of MtbFtsZ and its inhibitor which can be used for the design of potent anti-FtsZ agents as well as a virtual tool for screening of new lead from chemical library in the future.

MATERIALS AND METHODS

Preparation of MtbFtsZ and SRI-3072 structures

The structure of MtbFtsZ was retrieved from the protein data bank¹¹ (PDB code 1RLU) and then substrate GTP- γ -S was deleted from the protein

structure. The structure of MtbFtsZ inhibitor SRI-3072 was obtained from PubChem¹². Hydrogen and partial charge in molecular system of protein and ligand structures were assigned by CHARMM force field¹³. The energy minimizations were then performed with 5,000 steps of Steepest Descent (SD) followed by 5,000 steps of Adopted Basis-set Newton-Raphson (ABNR) using program Discovery Studio 2.5¹⁴.

Exploring binding site of Mtb-FtsZ

The minimized MtbFtsZ structure was used for exploring the potential active site. The possible binding sites were identified using “Find Site from Receptors Cavities” based on the shape of the receptor using program Discovery Studio 2.5. This technique helps to identify the binding pocket based on grid method¹⁵.

Docking Procedure

Docking calculations were performed with program LibDock¹⁶ implemented in Discovery studio 2.5. The 15Å site sphere for docking protocol was selected using coordinate in predefined binding site cavities. The 500 binding site features, so call “HotSpots” in binding site spheres were determined using a grid placed into the binding site with polar and apolar probes. The conformations of ligand poses were generated using BEST algorithm and then placed into binding site spheres based on triplets matching of hotspots. The docking poses were pruned and optimized. Finally, the LibDock score of each pose was calculated using a simple pair-wise method. The 30 top-ranked LibDock score poses were selected for calculation of binding energy between a receptor and a ligand¹⁷. *In situ* ligand-receptor minimization was performed on the complexes to remove any ligand van der Waals clashes prior to calculating the binding energy. The 5,000 steps of SD with free movement of atoms within the binding site sphere were used during the minimization. The complex pose with the best binding energy was kept for further calculations and analyses.

Optimization of MtbFtsZ–SRI-3072 complex and binding interaction analyses

The structure of MtbFtsZ–SRI-3072 complex was optimized by molecular dynamics (MD) simulation before binding site analysis. A set of minimization, heating, equilibration and production steps were performed using MD simulation with CHARMM force field¹³. Briefly, the minimization was carried out using 10,000 steps of conjugated gradient method. The Langevin dynamics in gas phase at 310K was consequently applied for MD simulation as follows: heating step for 10 ps, equilibration for 200 ps and final production for 2 ns. The non-bonded van der Waals and electrostatic forces were truncated at 14Å smoothly switching at 11 Å with time step 1 fs. All atoms were fully flexible except the protein backbone was kept in harmonic restraint with force constant of 20 kcal/mol. All steps in MD calculation were done using NAMD v2.7¹⁸.

The non-bonded interaction energies, *i.e.* van der Waals and electrostatic terms were calculated per-residue of amino acids within 4Å of SRI-3072. The residues which interact with the SRI-3072 were decorated using Ligand Binding Pattern (*i.e.* hydrogen bond donors and acceptors, and polar and nonpolar contacts involved in protein main-chain or side-chain atoms). 2D depiction of the SRI-3072 and its surrounding binding site residues was generated using Draw Ligand Interaction Diagram. Interactions, such as hydrogen bond, charge-charge interaction, and π interaction, between the surrounding residues and SRI-3072 were also displayed. Analysis of binding interaction and visualization were carried out using Discovery Studio 2.5 package. The calculations were performed on an Intel Corei7 2.66 GHz with 6 GB of RAM.

RESULTS AND DISCUSSIONS

1. Exploring the potential binding site of MtbFtsZ

The twelve possible binding pockets of MtbFtsZ (PDB code 1RLU after deleting

GTP- γ -S) were totally found using cavity search. In this study, only four major pockets were chosen for analyses (see Figure 1(c)). Since the dimer of MtbFtsZ composed of subunit A and B are nearly identical in structure⁸, the determined binding pocket #1 and #2 are nearly the same as pocket #3 and #4, respectively. It is interesting to note that the pocket #1 and #3 were located to the nucleotide recognition site of FtsZ, whereas pocket #2 and #4 were analogous to the Taxol-binding site of tubulin⁸. However, the coordinate of residues ranging from Arg60 to Gly69 and from Gly170 to Ala173 are disordered in structure of subunit B. Accordingly, only pocket #1 and #2 of subunit A were chosen for studies. This finding let us to speculate that SRI-3072 could undergo fill these pockets to inhibit the MtbFtsZ function.

2. Docking studies of SRI-3072 into MtbFtsZ

Molecular docking was performed to elucidate the binding mode of MtbFtsZ and SRI-3072. In this study, the structure of MtbFtsZ subunit A was used as target for docking SRI-3072 into nucleotide-binding pocket (pocket #1) and analogous taxol-binding pocket (pocket #2) using LibDock method.

2.1 Docking SRI-3072 into nucleotide binding pocket

Total of 82 binding poses were obtained from docking of SRI-3072 (Figure 1(a) and 1(b)) into nucleotide binding pocket (Pocket #1 in Figure 1(c)). The 30 top-ranked LibDock score poses were retained for binding energy calculation. The details of LibDock score and energy values of ligand poses with top-10 ranking of binding energy are listed in Table 1. Structures of MtbFtsZ–SRI-3072 complex docking into nucleotide binding site are shown in Figures 2(a) and 2(b). The MtbFtsZ–SRI-3072 complex of pose-25 yielded the highest binding energy of -98.05 kcal/mol (Figure 2 (c)). This complex structure was used for further analysis of binding interaction.

2.2 Docking SRI-3072 into analogous Taxol-binding site

The docking SRI-3072 into the Taxol-binding site (Pocket #2 in Figure 1) resulted in 82 ligand poses. Energies and LibDock scores of top-10 most binding energy ranking poses are summarized in Table 2. The MtbFtsZ–SRI-3072 complex of pose-3 produced the highest binding energy of -113.08 kcal/mol (Figure 3). This docked complex was used for analysis of binding interaction of SRI-3072 in analogous Taxol-binding pocket.

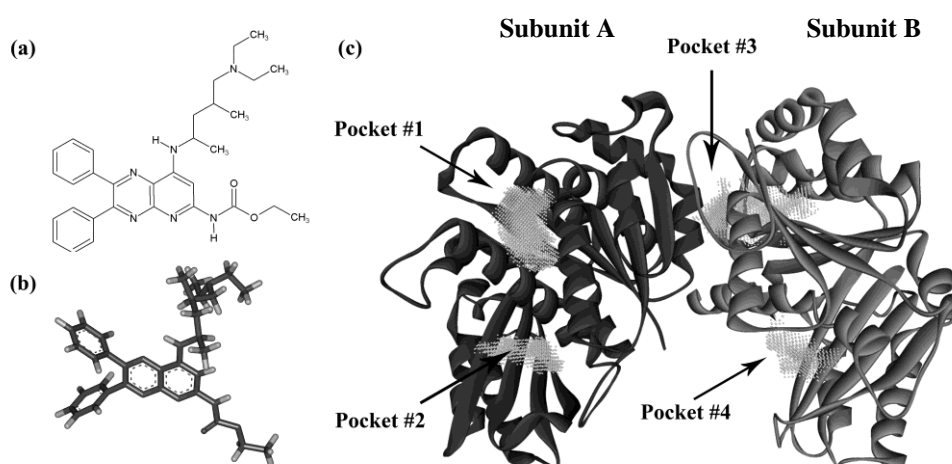


Figure 1. Structure of SRI-3072 and MtbFtsZ. (a), (b) 2D and 3D structures of SRI-3072, respectively, and (c) four major binding pockets of MtbFtsZ identified by “Find Sites from Receptor Cavities” in Discovery Studio 2.5.

Table 1. The top 10 most ranked binding energy (kcal/mol) and LibDock score of poses obtained from docking SRI-3072 complex into nucleotide-binding site MtbFtsZ.

Pose Number	Ligand Energy (kcal/mol)	Protein Energy (kcal/mol)	Complex Energy (kcal/mol)	Binding Energy (kcal/mol)	LibDock Score
25	33.33	-13,812.74	-13,877.46	-98.05	117.88
15	21.07	-13,819.27	-13,894.76	-96.57	120.57
38	17.97	-13,757.37	-13,832.52	-93.12	114.43
54	34.56	-13,810.62	-13,867.83	-91.76	110.06
13	13.07	-13,821.22	-13,896.47	-88.31	122.93
62	21.20	-13,820.17	-13,886.20	-87.23	107.03
18	19.61	-13,831.05	-13,897.66	-86.22	119.47
36	24.01	-13,831.72	-13,892.11	-84.40	114.60
97	14.89	-13,786.97	-13,854.88	-82.80	70.20
79	21.20	-13,821.27	-13,882.36	-82.30	99.36

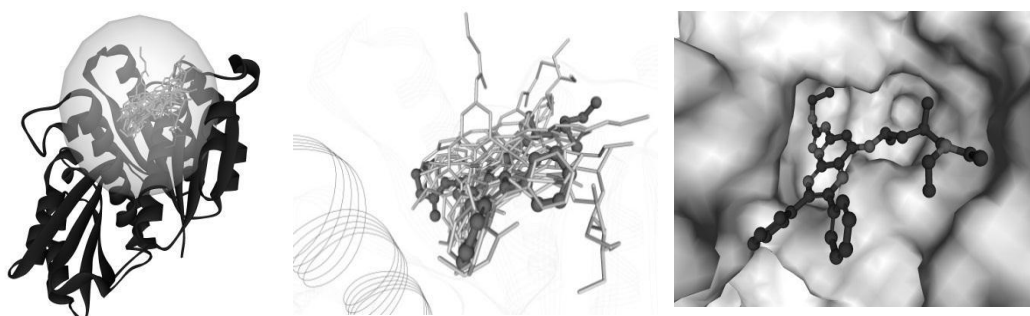


Figure 2. The MtbFtsZ–SRI-3072 complex at nucleotide binding site. (a), (b) The top 10 complex structures of MtbFtsZ and SRI-3072, (c) The MtbFtsZ–SRI-3072 complex pose-25 in nucleotide binding pocket. The structure representing as solid ribbon (MtbFtsZ), line ribbon (H7 helix), solid surface (nucleotide binding pocket), stick (docked poses of SRI-3072) and ball and stick (the best pose of SRI-3072).

Table 2. The top 10 most ranked binding energy (kcal/mol) and LibDock score of poses obtained from docking SRI-3072 complex into nucleotide-binding site MtbFtsZ.

Pose Number	Ligand Energy (kcal/mol)	Protein Energy (kcal/mol)	Complex Energy (kcal/mol)	Binding Energy (kcal/mol)	LibDock Score
3	29.94	-13,751.00	-13,834.10	-113.08	124.14
78	23.42	-13,737.70	-13,818.10	-103.84	76.16
12	21.50	-13,740.50	-13,821.50	-102.50	111.32
15	31.11	-13,727.40	-13,789.20	-92.95	106.09
19	29.50	-13,736.30	-13,797.70	-90.89	103.13
20	25.32	-13,723.40	-13,785.50	-87.41	102.81
21	21.67	-13,743.40	-13,807.40	-85.63	102.36
25	21.28	-13,740.60	-13,804.70	-85.36	100.64
8	15.33	-13,727.70	-13,796.20	-83.86	116.26
23	20.13	-13,754.70	-13,817.60	-83.04	102.01

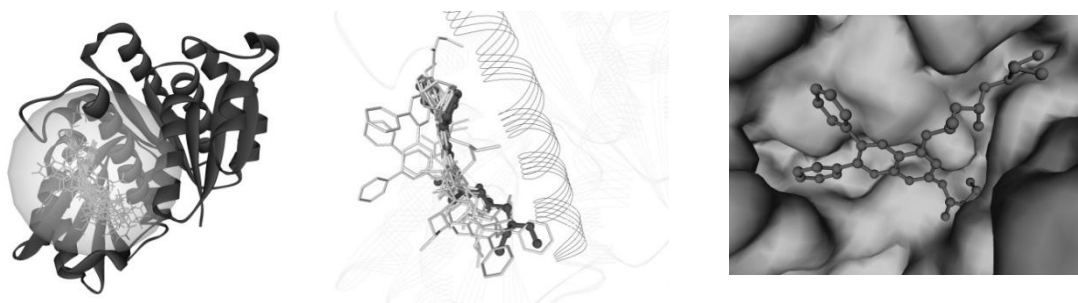


Figure 3. The MtbFtsZ–SRI-3072 complex at Taxol-binding site. (a), (b) The top 10 complex structures of MtbFtsZ and SRI-3072, (c) The MtbFtsZ–SRI-3072 complex pose-3 in Taxol-binding pocket. The structure representing as solid ribbon (MtbFtsZ), line ribbon (H7 helix), solid surface (Taxol-binding pocket), stick (docked poses of SRI-3072) and ball and stick (the best pose of SRI-3072).

3. Analysis of binding mode of SRI-3072 in complex with MtbFtsZ using molecular dynamics simulation

Structure models for MtbFtsZ–SRI-3072 docking complexes aided in understanding the binding mode of SRI-3072 in active site of MtbFtsZ. SRI-3072 was found to bind into two plausible active sites of MtbFtsZ, *i.e.* nucleotide-binding pocket and analogous Taxol-binding pocket. Since the flexibility of residues conformation in the receptor binding site is an important issue for analysis of ligand binding interaction, therefore, MtbFtsZ–SRI-3072 docking complexes were optimized by MD to relax the structure to equilibrium conformation. The results show that both complexes of SRI-3072 in nucleotide-binding pocket and in analogous Taxol-binding pocket reached the structural equilibrium at 2ns of MD simulation. This was confirmed by the plots of structural RMSD and energy, which indicate gradually reaching equilibrium with constant fluctuation of potential energy of the system (see Figures 4(a) and 4(b)).

The structure of MtbFtsZ–SRI-3072 complexes were selected from the last stable conformation of production step, and then minimized with 20,000 steps of conjugated gradient method before using as a final model for further investigation of binding interaction. The effect of MD simulation on structural rearrangement of protein and ligand were elucidated using RMSD deduced from structure

superimposition. The structures of MtbFtsZ–SRI-3072 complex obtained from docking and MD simulation were then compared by superimposing the structures (Figure 5). For nucleotide-binding complex, it is observed that the two structures displayed RMSD of 9.78Å and 3.95Å for whole protein and ligand, respectively. Whereas RMSD of 9.92Å and 2.75Å were respectively found for protein and ligand in Taxol-binding complex. The results indicate that such residues and ligand are quite flexible and therefore only results obtained from docking approach is not sufficient for using as analysis tool for elucidating the key interaction residues. The binding modes made by the stable structures of SRI-3072 with two binding sites after the molecular dynamics followed by minimization were suitable for inspection of binding interactions.

3.1 Binding mode analyses of SRI-3072 in the nucleotide binding site

Once the structure of SRI-3072 in nucleotide-binding site of MtbFtsZ was validated to be stable after MD simulation, it was further explored for binding mode of SRI-3072 and its binding interactions. The computed binding energy shows the value of -180.01 kcal/mol which is more stable than that of corresponding docked complex (*i.e.* -98.05 kcal/mol). Figure 6 and Table 3 summarize the interacting residues with within 4Å of SRI-3072 at nucleotide-binding pocket. The non-bonded van der Waals and electrostatic interactions

per-residue within 4Å of SRI-3072 are listed in Table 4. It is observed that SRI-3072 engages in hydrophobic interaction with several amino acids in the nucleotide-binding site along with hydrogen-bond interactions with Gly105 and Arg140. Side-chain of Arg140 formed hydrogen bond with carbonyl group (C=O) of ethyl carbamate moiety, whereas main-chain (peptide bond) of Gly105 formed hydrogen bond with nitrogen atom of tertiary amine chain of SRI-3072. The computed electrostatic interaction energies of Arg140 and Gly105 are -17.49 and -6.32 kcal/mol, respectively. The polar contacts were also observed for Gly18, Gly19, Asn22, Gly101, Thr106, Gly107 and Phe180 but with lower extents. Arg140 and Gly105 have been previously indicated to form hydrogen bonds to GTP- γ -S in MtbFtsZ 1RLU⁸. This conserved residue Arg140 (*i.e.* Arg169 in *M. jannaschii* FtsZ and Arg142

in *E. coli* FtsZ) has been required to accomplish a fully catalytically polymerizable conformation of FtsZ⁸. SRI-3072 was found to inhibit the GTPase activity by 20-25% at 100 μ M concentration⁶. The reduction of GTPase activity suggests that SRI-3072 may interfere with binding of inhibitor to the hydrophobic side chains of MtbFtsZ in the GTP binding pocket. However, the analysis of interaction residues has shown that the binding site of SRI-3072 probably lies in the neighborhood of GTP binding pocket of MtbFtsZ. The overlapping with a few hydrophobic residues of the active site of MtbFtsZ *i.e.* Pro132, Phe133 and Phe180 could be identified in this study. Thus, SRI-3072 probably binds to MtbFtsZ by hydrophobic interactions, overlapping with binding site of nucleotide and inhibits MtbFtsZ polymerization by interfering arrangement of the hydrophobic region of MtbFtsZ.

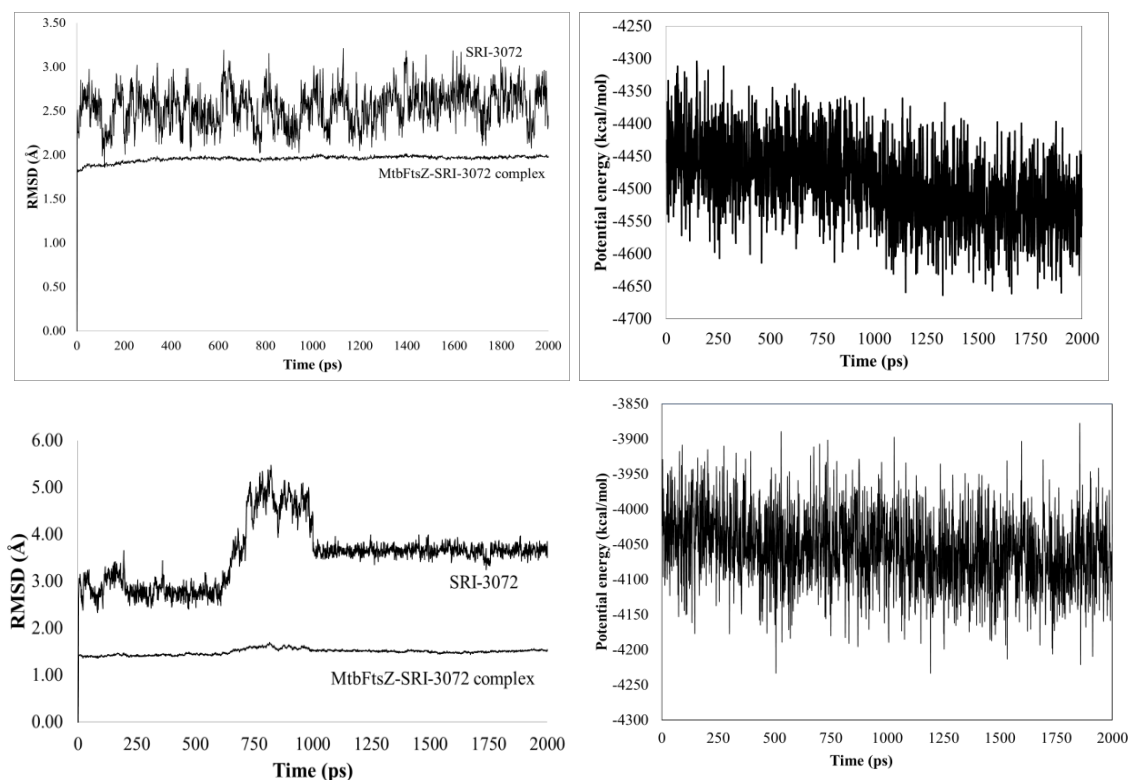


Figure 4. Plots of RMSD and energy along MD trajectory of MtbFtsZ–SRI-3072 complexes in nucleotide-binding pocket and (b) analogous Taxol-binding pocket.

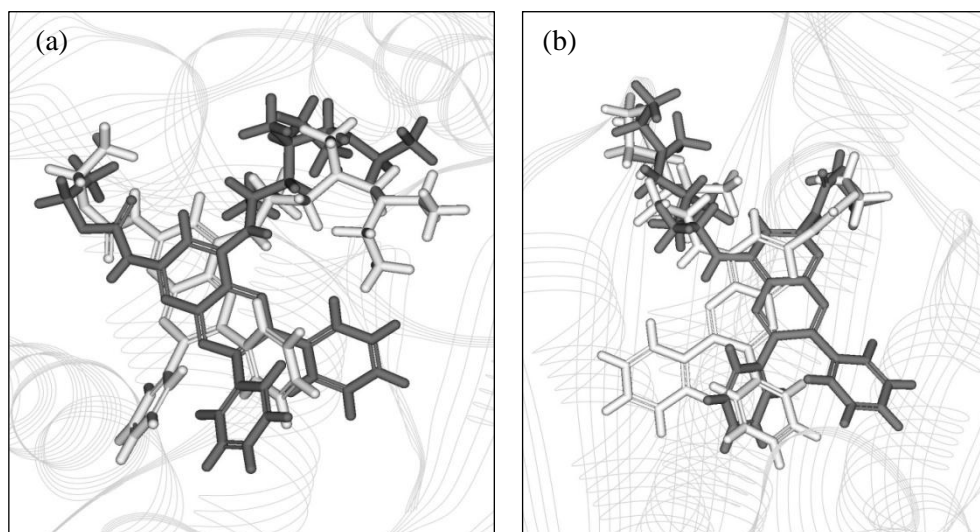


Figure 5. Superimposition of MtbFtsZ–SRI-3072 complex of docked conformer of SRI-3072 (shown as light gray) and equilibrium conformer of SRI-3072 after 2ns MD simulation (shown as dark gray) in (a) nucleotide-binding pocket and (b) analogous Taxol-binding pocket. MtbFtsZ shown as line ribbon.

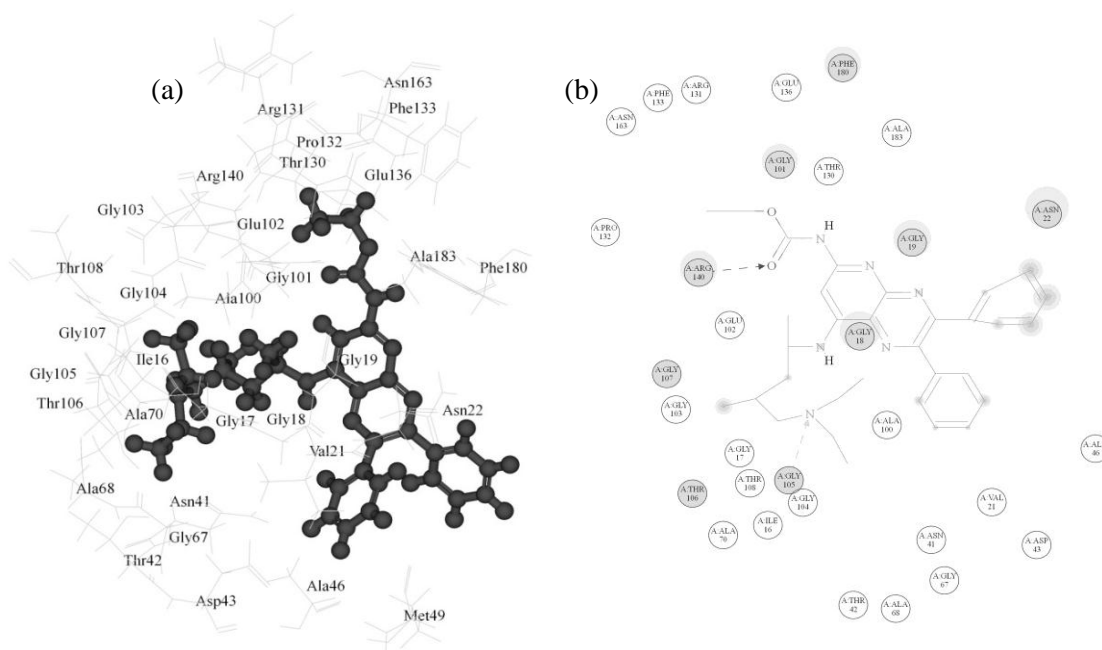


Figure 6. Binding mode of SRI-3072 in nucleotide-binding site. (a) 3D representation of interacting residues of MtbFtsZ (line) within a 4Å radius of SRI-3072 (ball and stick). (b) 2D interaction diagram of SRI-3072 (line) together with residues of MtbFtsZ within a 4Å radius representing as hydrogen-bonded, charge or polar interacting residues (gray circles) and van der Waals interacting residues (white circles). Hydrogen-bond interactions represented by a dashed line with an arrow head directed towards the electron donor atom.

Table 3. Type of binding interactions defined for each interacting residues in nucleotide-binding pocket within 4Å of SRI-3072 binding.

Binding interaction	Residue
Hydrogen bond donor	
• Main-chain	Gly105
• Side-chain	Arg140
Polar contact	
• Main-chain	Gly18, Gly19, Gly101, Gly105, Thr106, Gly107, Phe180
• Side-chain	Asn22, Arg140
Nonpolar contact	
• Main-chain	Ile16, Gly17, Gly18, Gly19, Asn22, Ala46, Gly67, Ala68, Ala70, Gly101, Glu102, Gly103, Gly104, Gly105, Thr106, Gly107, Thr130, Arg131, Pro132
• Side-chain	Val21, Asn22, Asp43, Ala46, Met49, Ala68, Ala70, Ala100, Thr106, Thr130, Pro132, Phe133, Arg140, Asn163, Phe180, Ala183

3.2 Binding mode analysis of SRI-3072 in the analogous Taxol-binding site

The analogous Taxol-binding site of MtbFtsZ was also investigated to locate the possible binding mode between SRI-3072 and interacting residues within this pocket. The binding energy of -160.01 kcal/mol was found in optimized complex, while -113.08 kcal/mol was found in docked complex. The amino acid residues within 4Å of SRI-3072 at Taxol-binding pocket are depicted in Figure 7 and corresponding binding interaction are summarized in Table 5. The van der Waals and electrostatic interaction energies per-residue are listed in Table 6 based on amino acids located within 4Å of SRI-3072 inhibitor. The results show that hydrophobic interactions mainly engage the binding mode of SRI-3072 in this region with the van der Waals interaction energy of -57.82 kcal/mol. The cation- π interaction was detected in the vicinity of

phenyl ring orientation of SRI-3072 to the side-chain of Arg181. SRI-3072 is predicted to bind in a hydrophobic channel formed by Leu166, Met169, Leu188, Met223, Ile225, Leu246, Leu299 and Val305. The electrostatic interactions were also observed within this putative binding cleft. The side-chain of Asn189 and main-chain of Gly226 are hydrogen-bonded to the ethyl carbamate portion of SRI-3072 with electrostatic interaction energy of -10.57 and -4.56 kcal/mol, respectively. This region was previously declared as a part of the Taxol-binding site of tubulin and has been suggested to alter the inter-domain orientations of tubulin and FtsZ¹⁹⁻²¹. Accordingly, the binding mode of SRI-3072 in this active site probably contributes to the inhibition of GTPase activity and MtbFtsZ polymerization. The putative Taxol-binding region has been reported for mapping the binding site of compound PC190723, a potent anti-FtsZ activity against *B. subtilis* and *S. aureus*²².

Table 4. Interaction energy (per-residue) of amino acid in nucleotide-binding pocket within 4Å of SRI-3072 binding.

Residue	Interaction Energy (kcal/mol)	VDW Interaction Energy (kcal/mol)	Electrostatic Interaction Energy (kcal/mol)
Ile16	-0.47	-0.68	0.20
Gly17	-2.70	-2.23	-0.47
Gly18	-7.41	-6.00	-1.42
Gly19	-5.04	-3.39	-1.65
Val21	-6.53	-0.92	-5.61
Asn22	-3.15	-3.98	0.82
Asn41	0.99	-1.51	2.51
Thr42	-4.48	-0.80	-3.67
Asp43	-2.04	-1.31	-0.73
Ala46	-1.65	-0.63	-1.02
Met49	-1.13	-1.12	-0.01
Gly67	-0.68	-1.27	0.59
Ala68	0.49	-1.44	1.93
Ala70	-3.98	-2.34	-1.64
Ala100	-0.69	-0.43	-0.26
Gly101	-2.41	-3.38	0.97
Glu102	-3.46	-1.78	-1.68
Gly103	-1.11	-1.10	-0.01
Gly104	-6.80	-2.57	-4.22
Gly105	-8.24	-1.92	-6.32
Thr106	-3.86	-3.52	-0.34
Gly107	0.67	-1.33	2.01
Thr108	-4.47	-0.53	-3.94
Thr130	-1.40	-1.32	-0.08
Arg131	3.56	-0.55	4.11
Pro132	-1.09	-2.30	1.21
Phe133	1.59	-1.39	2.98
Glu136	-2.60	-0.59	-2.00
Arg140	-19.87	-2.38	-17.49
Asn163	-2.78	-1.46	-1.32
Phe180	-4.74	-3.64	-1.10
Ala183	-3.58	-1.44	-2.14
Total	-99.02	-59.26	-39.77

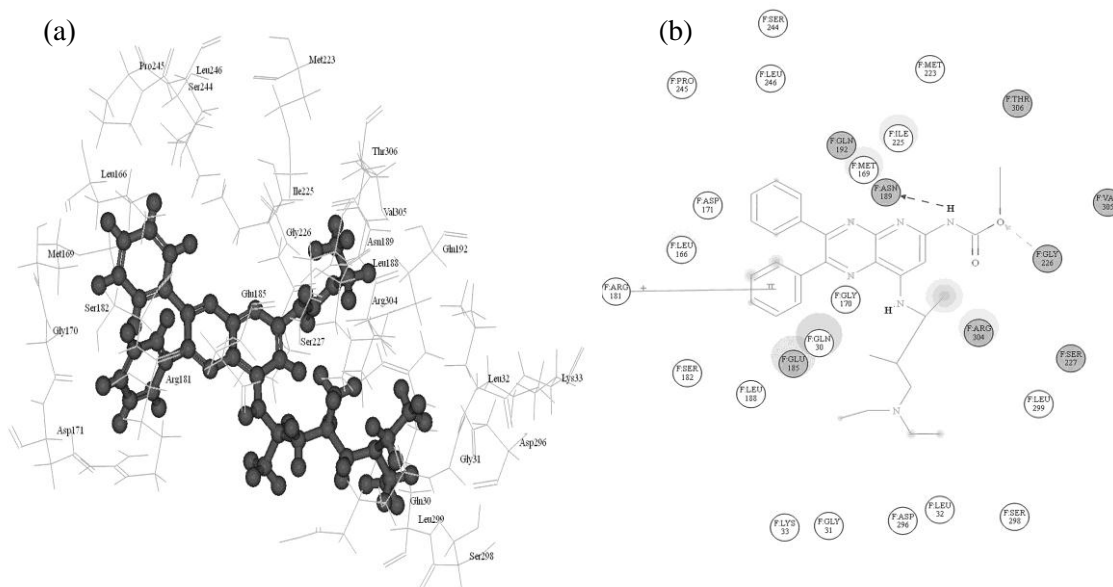


Figure 7. Binding mode of SRI-3072 in analogous Taxol-binding site. (a) 3D representation of interacting residues of MtbFtsZ (line) within a 4Å radius of SRI-3072 (ball and stick). (b) 2D interaction diagram of SRI-3072 (line) together with residues of MtbFtsZ within a 4Å radius representing as hydrogen-bonded, charge or polar interacting residues (gray circles) and van der Waals interacting residues (white circles). Hydrogen-bond interactions represented by a dashed line with an arrow head directed towards the electron donor atom. Cation- π interactions shown as line with symbols indicating the interaction.

Table 5. Type of binding interactions defined for each interacting residues in analogous Taxol-binding pocket within 4Å of SRI-3072 binding.

Binding interaction	Residue
Hydrogen bond donor	
• Main-chain	Gly226
Hydrogen bond acceptor	
• Side-chain	Asn189
Polar contact	
• Main-chain	Gly226, Ser227, Val305
• Side-chain	Glu185, Asn189, Gln192, Arg304, Thr306
Nonpolar contact	
• Main-chain	Gln30, Gly31, Leu166, Met169, Gly170, Asp171, Ser182, Asn189, Ile225, Gly226, Ser298, Leu299, Arg304, Val305, Thr306
• Side-chain	Gln30, Leu166, Met169, Asp171, Ser182, Glu185, Leu188, Asn189, Gln192, Met223, Ile225, Pro245, Leu246, Asp296, Ser298, Leu299, Arg304, Thr306

Table 6. Interaction energy (per-residue) of amino acid in analogous Taxol-binding pocket within 4Å of SRI-3072 binding.

Residue	Interaction Energy (kcal/mol)	VDW Interaction Energy (kcal/mol)	Electrostatic Interaction Energy (kcal/mol)
Gln30	-2.40	-3.18	0.78
Gly31	-0.96	-1.57	0.62
Leu32	1.39	-0.33	1.71
Lys33	2.95	-0.44	3.38
Leu166	-3.04	-1.90	-1.14
Met169	-2.27	-2.31	0.05
Gly170	-3.00	-1.98	-1.02
Asp171	-3.82	-1.03	-2.79
Arg181	-3.19	-1.50	-1.69
Ser182	-2.69	-0.98	-1.71
Glu185	-7.14	-5.11	-2.03
Leu188	-2.68	-1.14	-1.54
Asn189	-14.71	-4.14	-10.57
Gln192	-6.97	-3.58	-3.39
Met223	-0.81	-0.41	-0.40
Ile225	-7.77	-5.55	-2.22
Gly226	-6.83	-2.27	-4.56
Ser227	0.45	-1.51	1.96
Ser244	-3.01	-0.42	-2.59
Pro245	-0.74	-0.74	0.00
Leu246	-1.74	-1.56	-0.18
Asp296	-5.41	-1.51	-3.90
Ser298	1.07	-1.21	2.27
Leu299	-1.41	-1.55	0.15
Arg304	-11.01	-9.02	-1.99
Val305	-1.86	-1.92	0.06
Thr306	-2.85	-0.95	-1.91
Total	-90.45	-57.82	-32.64

The results of binding mode analyses of SRI-3072 provide pertinent information that SRI-3072 is preferable to bind with the nucleotide-binding site as observed by the existence of more stable in binding energy and interaction energy than those found in Taxol-binding site.

CONCLUSION

Tuberculosis is one of the worldwide infectious diseases along with the problem of multidrug resistance *Mycobacterium tuberculosis*. The discovery and development

of anti-TB drug with new mechanism of action is urgent need to overcome the problem of TB disease. The bacterial cell-division protein FtsZ has been revealed as the potential target for discovery of new anti-TB agents. Among all FtsZ inhibitors, the SRI-3072 has exhibited anti-TB activity by inhibition of GTPase activity and polymerization of MtbFtsZ. Our study predicted the binding site and binding mode of SRI-3072 in MtbFtsZ. The possible binding sites were initially defined by cavity detection analysis of MtbFtsZ

structure. Two plausible binding pockets were chosen, *i.e.* nucleotide-binding pocket and analogous Taxol-binding pocket. The SRI-3072 was docked into those binding pockets and the best docked poses were selected based on ranked LibDock score and binding energy analysis. The docked complexes were then submitted for molecular dynamics simulation to retrieve the stable structures. Residues involved in binding interactions were allocated together with their interaction energies. The hydrogen bonding and hydrophobic interactions with active site residues presented here validate the binding mode of SRI-3072 in both binding site. However, the preferable binding mode of SRI-3072 is in nucleotide-binding site because its binding energy and interaction energy are higher than those observed in Taxol-binding pocket. Our results insight into structural information which can further be exploited to design selective inhibitors of *M.tuberculosis* FtsZ based on SRI-3072 derivatives.

ACKNOWLEDGEMENTS

The authors wish to thank the Research, Development and Engineering (RD&E) fund through the National Nanotechnology Center (NANOTEC), National Science and Technology Development Agency (NSTDA), Pathumthani, Thailand (project no.NN-B-22-EN8-15-51-23) for research funding.

REFERENCES

1. Bramhill D. Bacterial cell division. *Annu Rev Cell Dev Biol* 1997; 13:395-424.
2. Lutkenhaus J, Addinall SG. Bacterial cell division and the Z ring. *Annu Rev Biochem* 1997; 66:93-116.
3. Romberg L, Levin PA. Assembly dynamics of the bacterial cell division protein FtsZ: poised at the edge of stability. *Annu Rev Microbiol* 2003; 57: 125-154.
4. De Boer PCR, Rotherfield L. The essential bacterial cell-division protein FtsZ is a GTPase. *Nature*; 359:254-256.
5. Kumar K, Awasthi D, Berger WT, Tonge PJ, Slayden RA, and Ojima I. Discovery of anti-TB agents that target the cell-division protein FtsZ. *Future Med Chem* 2010; 2(8): 1305-1323.
6. White EL, Suling WJ, Ross LJ, Seitz LE, Reynolds RC. 2-alkoxycarbonyl-aminopyridines: inhibitors of Mycobacterium tuberculosis FtsZ. *J Antimicrob Chemother* 2002; 50(1):111-114.
7. Reynolds RC, Srivastava S, Ross LJ, Suling WJ, White EL. A new 2-carbamoyl pteridine that inhibits mycobacterial FtsZ. *Bioorg Med Chem Lett* 2004; 14(12): 3161-3164.
8. Leung AKW, White EL, Ross LJ, *et al.* Structural of *Mycobacterium tuberculosis* FtsZ reveals unexpected, G protein-like conformational switches. *J Mol Biol* 2004; 342:953-970.
9. Oliva MA, Trambaiolo D and Löwe J. Structural insights into the conformational variability of FtsZ. *J Mol Biol* 2007; 373: 1229-1242.
10. Lu C, Stricker J, Erickson HP. Site-specific mutations of FtsZ-effects on GTPase and in vitro assembly. *BMC Microbiol* 2001; 1(7).
11. Protein data bank PDB. www.pdb.org (accessed July 2011).
12. PubChem. www.pubchem.ncbi.nlm.nih.gov (accessed July 2011).
13. CHARMM. www.charmm.org (accessed July 2011).
14. Accelrys Inc. (2010) Discovery Studio 2.5. Accelrys Inc., San Diego.
15. Venkatachalam CM, Jiang X, Oldfield T, Waldman M. LigandFit: a novel method for the shape-directed rapid docking of ligands to protein active sites. *J. Mol. Graph. Model* 2003; 21:289-307.
16. Rao SN, Head MS, Kulkarni A, and Lalonde JM. Validation studies of the site-directed docking program LibDock. *J Chem Inf Model* 2007; 47(6):2159-2171.
17. Tirado-Rives J, Jorgensen WL. Contribution of conformer focusing to the uncertainty in predicting free energies for protein-ligand binding. *J Med Chem* 2006; 49: 5880-5884.
18. Phillips JC, Braun R, Wang W, Gumbart J, Tajkhorshid E, Villa E, Chipot C, Skeel RD, Kalé L, Schulten K. Scalable molecular dynamics with NAMD. 2005; 26(16).
19. Löwe J and Amos LA. Crystal structure of the bacterial cell-division protein FtsZ. *Nature* 1998; 391:203-206.
20. Nogales E, Wolf SG and Downing KH. Structure of the $\alpha\beta$ tubulin dimer by electron crystallography. *Nature* 1998; 391:199-203.
21. Löwe J and Amos LA. How Taxol stabilises microtubule structure. *Chem & Biol* 1999; 6:R65-R69.
22. Haydon DJ, Stokes NR, Ure R, *et al.* An inhibitor of FtsZ with potent and selective

anti-staphylococcal activity. *Science* 2008;
321:1673-1675.